AD_____

Award Number: MIPR 1GCDGB1102

TITLE: Evaluation of Chronic Stress Induced Neurodegeneration and Treatment using an In-vivo Retinal Model

PRINCIPAL INVESTIGATOR: Heike K. Rentmeister-Bryant, Ph.D.

CONTRACTING ORGANIZATION: Naval Health Research Center
Brooks AFB, TX 78235-5665

REPORT DATE: September 2004

TYPE OF REPORT: Final

PREPARED FOR: U.S. Army Medical Research and Materiel Command
Fort Detrick, Maryland 21702-5012

REPORT DOCUMENTATION PAGE

Form Approved
OMB No. 074-0188

1. AGENCY USE ONLY (Leave blank)	2. REPORT DATE	3. REPORT TYPE AND DATES COVERED
	September 2004	Final (1 May 2001 - 30 Sep 2004)

4. TITLE AND SUBTITLE
Evaluation of Chronic Stress Induced Neurodegeneration and Treatment using an In-vivo Retinal Model

5. FUNDING NUMBERS
MIPR 1GCDGB1102

6. AUTHOR(S)

Heike K. Rentmeister-Bryant, Ph.D.

7. PERFORMING ORGANIZATION NAME(S) AND ADDRESS(ES)

Naval Health Research Center
Brooks AFB, TX 78235-5665

E-Mail: Heike.Rentmeister-Bryant@navy.brooks.af.mil

8. PERFORMING ORGANIZATION REPORT NUMBER

9. SPONSORING / MONITORING AGENCY NAME(S) AND ADDRESS(ES)
U.S. Army Medical Research and Materiel Command
Fort Detrick, Maryland 21702-5012

10. SPONSORING / MONITORING AGENCY REPORT NUMBER

11. SUPPLEMENTARY NOTES

12a. DISTRIBUTION / AVAILABILITY STATEMENT
Approved for Public Release; Distribution Unlimited

12b. DISTRIBUTION CODE

13. ABSTRACT (Maximum 200 Words)

The objective of this project is to develop an *in vivo* damage model for the study of the mechanisms underlying retinal injuries and other neurodegenerative disorders. For this purpose the small snake eye with its unique suite of ocular properties, combined with the imaging capabilities of the confocal Scanning Laser Ophthalmoscope model was selected. Progress has been made in three areas of research necessary to establish the snake eye as a model for human neural injury/disease: (1) Morphology: Photochemical lesions are difficult to produce, are visible primarily at 24-hrs post-exposure, and therefore leave no experimental end point to be improved by treatment; (2) Electrophysiology: The functional characteristics of the pattern-evoked electroretinogram (PERG) recorded from the normal rat snake eye have been documented, and initial experiments with laser exposures indicate that the PERG is capable of tracking laser-induced changes in retinal function; and (3) Immunohistochemical analyses: Further evidence has been documented that the rat snake has an all cone retina. Immunohistochemical methods provide an additional tool for identifying key proteins released in response to neural injury.

14. SUBJECT TERMS
Neurodegeneration, Retinal injury, Retinal function, Snake eye, Laser, Photoreceptor, confocal Scanning Laser Ophthalmoscope

15. NUMBER OF PAGES
31

16. PRICE CODE

17. SECURITY CLASSIFICATION OF REPORT	18. SECURITY CLASSIFICATION OF THIS PAGE	19. SECURITY CLASSIFICATION OF ABSTRACT	20. LIMITATION OF ABSTRACT
Unclassified	Unclassified	Unclassified	Unlimited

Table of Contents

INTRODUCTION

The objective of this project is to develop an *in vivo* damage model for the evaluation of the mechanisms underlying neurodegeneration in the retina following thermal and/or photochemical laser injuries. For this purpose the small snake eye model was selected with its unique suite of ocular properties, which include the ability to image retinal structures in cellular detail (Figure 1) through the natural pupil using the confocal Scanning Laser Ophthalmoscope (cSLO). The cSLO/snake eye model has the advantage that we can observe in the same subject cellular level changes over time in an all cone retina, while subjects require only light anesthesia. These SLO images are equivalent in some ways, to histological samples from the eyes of other retinal injury models (commonly used are monkey, rabbit, rat, and mouse models).

In order to establish the cSLO/snake eye model for the study of neurodegeneration and human disease, we continue to study the properties of the snake eye model as well, in order to understand the differences and similarities to other vertebrate eyes, as they pertain to retinal injury. Thus, as we examine retinal injury in the snake eye we are also collecting background data on the snake's visual system. Ultimately, it is hoped that this damage model can be transitioned for the investigation of a number of neurodegenerative disorders, such as Parkinson's disease.

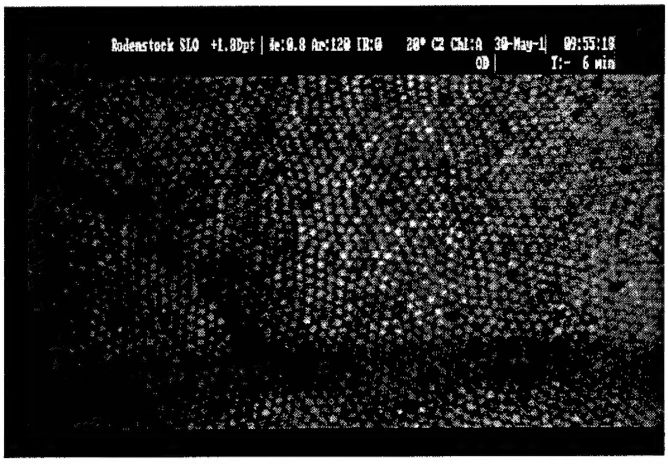

Figure 1: Photoreceptor matrix of an intact *in vivo* rat snake eye, imaged with a cSLO. This is an all cone retina, similar in this respect, to the human macula. Cell spacing is ~ 10-12 μ.

In the previous work period in this project, the structure and function of the retina of the Great Plains rat snake (*Elaphe guttata emoryi*) were characterized. The salient findings from the previous period were: (1) the retina of this animal appeared to contain only cone photoreceptors, (2) the high numerical aperture of the eye (a function of its small size and high magnification factor) enabled the photoreceptor matrix to be imaged with standard ophthalmic instrumentation such as the scanning laser ophthalmoscope, and (3) an electrophysiological measure of retinal function, the pattern-evoked electroretinogram (PERG) could be recorded from the animal *in vivo* (Rentmeister-Bryant et al., 2002; 2003). The ability to image individual photoreceptors and to characterize the function of the retina with an objective electrophysiological measure was the justification for using the snake as an experimental model for laser ocular bioeffects research.

BODY

Our work with this damage model follows three general areas:

I. Morphological examination of retinal injury and treatment;
II. Electrophysiological assessment of visual function in the snake small eye model following laser exposure; and
III. Immunohistochemical analyses of snake retina.

I. Morphological examination of photochemical retinal injury and treatment

Over the past twelve months, this laboratory has continued experiments with short wavelength visible laser exposures in the cSLO/snake eye model with the anticipation that the resultant photochemical injury might be a better model for chronic neurodegeneration than the thermal retinal injury model previously established. Photochemical retinal laser injuries differ from thermal ones in that they are produced by low energy levels, longer exposure times, and only with shorter wavelengths.

To investigate photochemical retinal laser injuries, a diode-pumped, solid state, Neodymium-VO_4 laser emitting at 473 nm (Intelite BM73) was mounted and aligned coaxially to the imaging beam of the cSLO (Rodenstock Model 101). The exposure beam was expanded slightly to give a retinal spot size of approximately 50 μm. The exposure duration was controlled with a mechanical shutter that interrupted the beam. Animals (Great Plains rat snakes: *Elaphe guttata emoryi*) were anesthetized with an intra-peritoneal injection of a ketamine / xylazine cocktail, in a ratio of 3.5:1 respectively, at an approximate dose of 50-75 mg/kg. Previously, it was established that this ketamine/ xylazine cocktail gives good oculostasis for short laser exposures and eye examinations in these animals. However, oculostasis was problematic during several of the present experiments, in which exposure durations were greater than 10 seconds, and resulted in slow eye movements affecting alignment of the laser spot on the retina.

After several sessions titrating laser dosimetry to produce observable retinal effects, it was determined that no effects were seen at laser powers below 2.5 mW, at any feasible exposure duration. The effects seen at 5 mW laser power became consistent at 10 sec exposures (see Graphs 1-3 below, which show the results of exposures from two series of 5mW, 473nm laser beam exposures). Table 1 shows the exposure results for 5 mW laser power at various exposure durations for all examination times, three of which are depicted in Graphs 1-3 below.

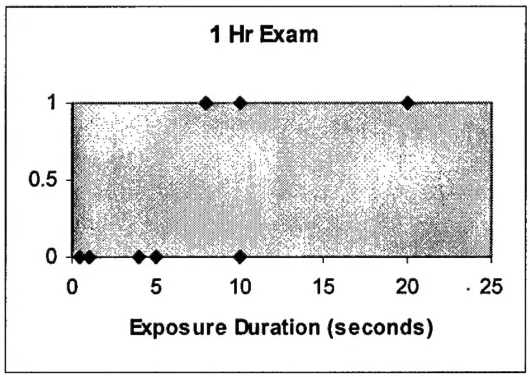

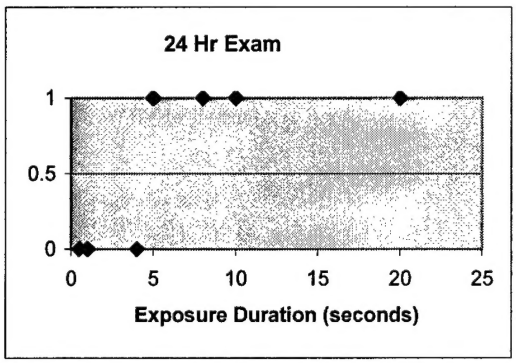

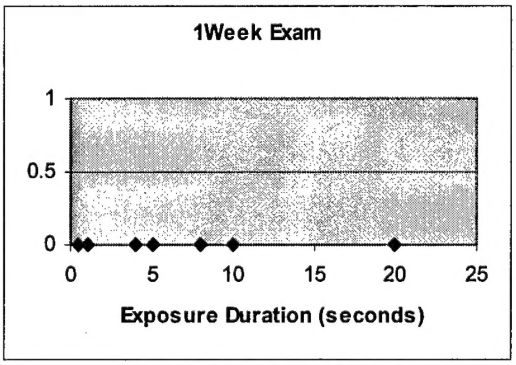

Graphs 1-3: Results of laser dosimetry: several 473nm laser exposure durations at 5mW. Only the three most relevant (1hr, 24hrs, 1-wk) of the six examination times recorded are displayed. Results of exposures are scored here as either 0 (=no observable lesion) or 1 (=observable lesion) against duration of exposure (sec). The displayed data points are from two separate exposure sessions, and consist of 15 total exposures.

5 mW 473 nm Exposures	Exam Time					
Exposure Duration in seconds	1hr	4 hr	6 hr	24 hr	30 hr	1week
0.5	-	-	-	-	-	-
1	-	-	-	-	-	-
1	-	-	-	-	-	-
4	-		-	-		-
4	-		-	-		-
5	-	-		+	+	-
8	+		+	+		-
10	-	-	+	+	+	-
10	+		+	+		-
10	+		+	+		-
10	+		+	+		-
20	+	-	+	+	+	-
20	-	-	+	+	+	-
20	-	-	+	+	+	-
20	-	-	+	+	+	-

Table 1: Exposure results @ various examination times for 5 mW laser power exposures. Note: Shaded columns are graphically displayed above. "+"= visible lesion; "-"= non-observable lesion.

The observed laser effects were characterized by small (50-75 μm) light areas in the cSLO's retinal view. Lesions were best observed using the IR illumination beam and were faint or absent when viewed using the HeNe (Red) and Argon (both Green and Blue) illumination beams (Figures 2 A&B). Similarly, the images were most easily viewed at deeper focal planes (more posterior retina), and were often not visible in the photoreceptor level or above. Often the lesions were not immediately apparent, but most developed at exposure sites in an hour. Some required as much as 6-hrs post exposure to develop. At 24-hrs post, these lesions were consistently visible. On longer follow-up examination (1-2 weeks post exposure), these lesions were either no longer visible or much reduced in size. In none of these lesions was there any observable loss of photoreceptors at the lesion sites.

A

B

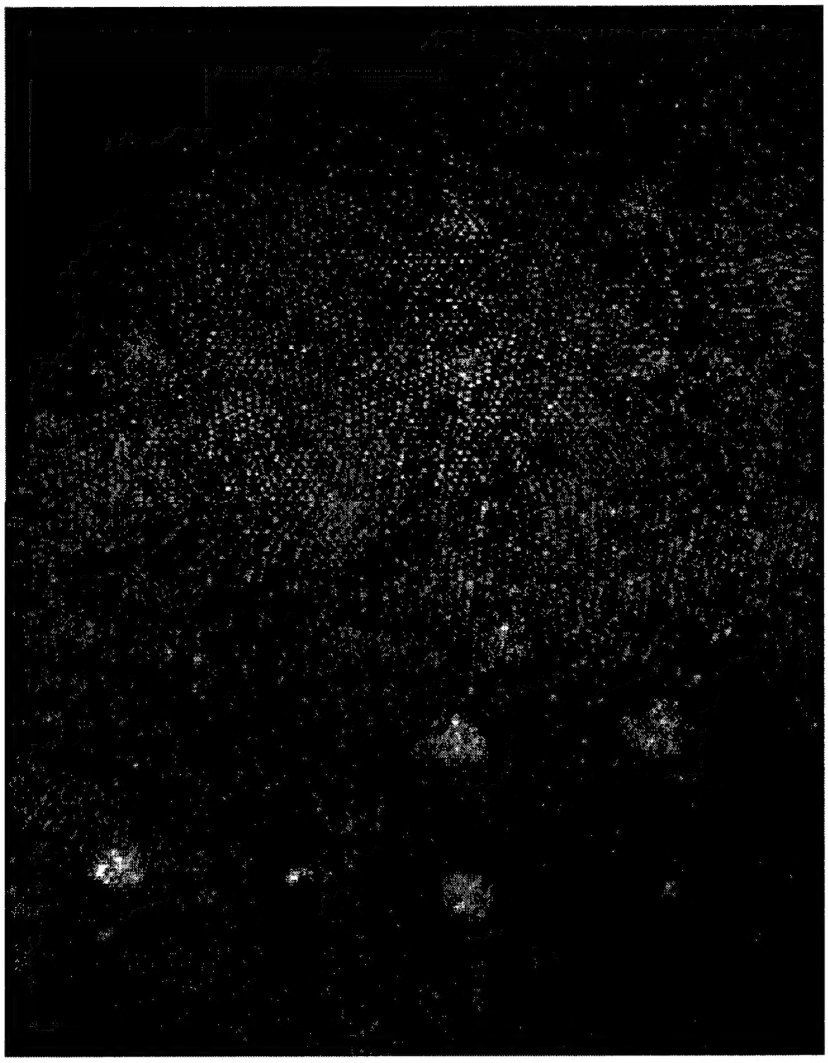

Figure 2 A&B: cSLO images of short wavelength lesions in the rat snake retina.
Fig. 2A: 40° HeNe illuminated cSLO image, 24-hrs post-exposure.
Fig. 2B: Same pattern of lesions illuminated with the cSLO's infrared laser, 24-hrs post-exposure.
Note the increased visibility of the lesions with IR illumination.

Next it was attempted to determine if the photochemical damage in the retinae of these animals could be measured using fluorescent dyes, which are biochemical markers for oxidative stress in the cell. Two different dyes, either 2',7'-dichlorodihydrofluorescein diacetate (Molecular Probes D-399) or carboxy-2',7'-dichlorodihydrofluorescein diacetate (Molecular Probes C-400), were administered in different animals via intra-cardiac injection, 30 minutes post-exposure. This laboratory used the same technique after thermal retinal injury in the snake eye, and observed distinct fluorescence at exposure sites and (with the C-400 dye) fluorescent white blood cells moving toward the injury site (Rentmeister-Bryant et al., 2002). In the case of these low-level, short wavelength exposures, however, only faint and blurry fluorescence marked the lesion sites (with either dye), and leucocytes were not seen in any views. In attempts to quench the oxidative stress with additional administration of N-acetylcysteine (NAC), no observable difference between dye + NAC and Dye alone was noted (procedures were described previously; Rentmeister-Bryant et al., 2002).

A total of five Great Plains rat snakes were used in these experiments. Three subjects were used more than once (in the case of Ege-014 both eyes were exposed; subjects Ege-016 and Ege-018 received multiple exposures in the same eye).

Of the three main retinal laser injury mechanisms (thermal, Q-switched/mechanical and photochemical), the injury modality we examined here, that of photochemical retinal injury, is the least well known. The effects of using this laser in this model, while interesting and deserving of more study, do not appear to lend themselves to treatment studies. The lack of observable permanent cellular deficits leaves no experimental end point to be improved by treatment.

II. Electrophysiological assessment of visual function in the snake small eye model following laser exposure

In this section, the work with the pattern-evoked electroretinogram (PERG) recorded from the rat snake will be reported. The functional characteristics of the PERG recorded from the normal snake eye have been documented, and initial experiments with laser exposures will be described, which indicate that the PERG is capable of tracking laser-induced changes in retinal function. The laser available during this period, however, was not capable of producing sufficient retinal irradiance to induce a permanent lesion; consequently the functional changes detected by the PERG were transient. A more powerful laser has just been installed in the laboratory, and the next phase of experiments will document the effects of permanent laser lesions.

Methods:

Four Great Plains rat snakes (*Elaphe guttata emoryi*) were studied. Animals were anesthetized with an intra-peritoneal injection of ketamine/xylazine, in a ratio of 3.5:1 respectively, at an approximate dose of 50-75 mg/kg (for the drug combination). Additional anesthetic was administered in 10 mg/kg doses as required, in order to maintain the animals in a state suitable for electrophysiological recording. A Rodenstock confocal scanning laser ophthalmoscope (cSLO, Model 101) was used to image the snake retina. Animals were placed in a custom-made holder that allowed their eyes to be positioned at the aperture of the cSLO. A schematic drawing of the imaging and recording arrangement is shown in Figure 3. The cSLO was outfitted with a HeNe laser (which provided visible stimulation with red light), and with an infrared diode laser that enabled imaging the fundus with invisible light.

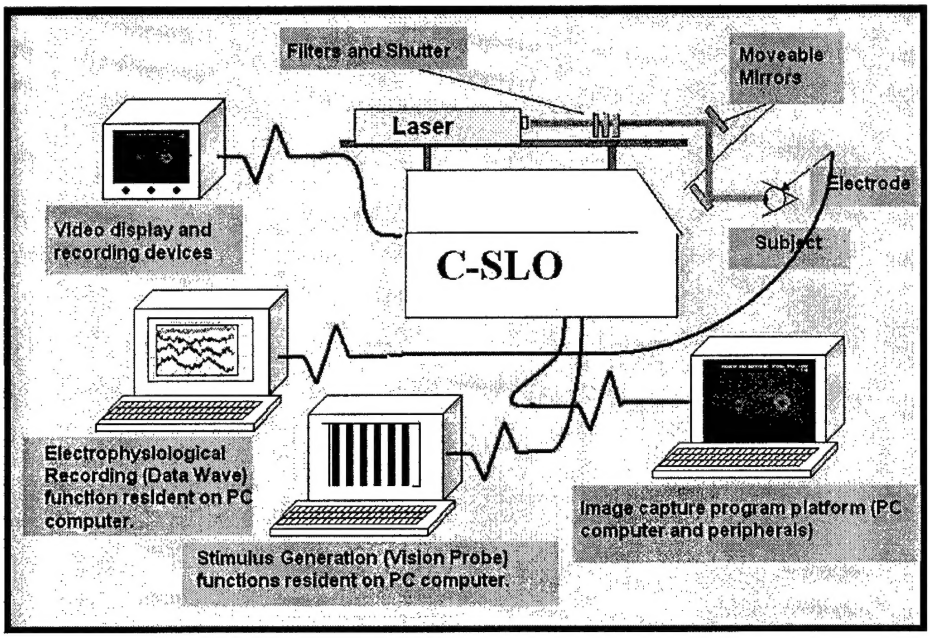

Figure 3. A block diagram of the visual stimulation and recording system used to obtain PERG responses from anesthetized rat snakes. The stimulator shown in this diagram is the cSLO, which could produce gratings internally projected into the animal's eye. External stimulation, with the snake viewing counterphasing square wave gratings on a CRT, was also used.

Electroretinographic responses were elicited with 99% contrast, counterphased square wave gratings projected on to the snake's retina. The stimulus gratings themselves were generated by a computer-based visual stimulator (VisionProbe®, San Antonio, TX). The stimulus gratings were presented in two ways: internally via the cSLO, or externally on a CRT that the snake viewed at a distance of 21 cm. To produce the stimulus gratings via the cSLO, the VisionProbe controlled the acousto-optical modulator of the cSLO, which in turn drove the cSLO's HeNe laser (632.8 nm) to produce the grating stimuli directly on the animal's retina. During visual stimulation, the retina was simultaneously imaged with the cSLO to ensure that the eye was stable during the electro-physiological recording period. For external viewing, the snake's head was oriented at about a 20-degree angle to the CRT, an arrangement, which empirically was found to produce the greatest amplitude PERG. The external display was able to present a wider range of stimulus spatial and temporal frequencies than could be generated by the cSLO imaging circuitry, however, it was easier to incorporate the laser into the optical apparatus with the SLO.

A diode-pumped, solid state, Neodymium-VO_4 laser emitting at 473 nm (Intelite BM73) was mounted and aligned coaxially to the imaging beam of the cSLO. The beam was regulated to deliver 10 mW. The exposure duration was controlled with a mechanical shutter that interrupted the beam.

In order to record the PERG from the eye, a small incision was made in the spectacle (the clear, specialized patch of skin covering the snake's eye) near the limbus of the eye. This was accomplished without injuring the cornea. The tip of a Grass needle electrode was placed into the incision. Electrical contact was improved by occasionally applying a drop of Ringer's solution onto the electrode tip-tissue junction.

Electrophysiological responses were amplified using a Grass Neurodata 12 amplifier with frequency bandpass limits set from .1 to 1 KHz. Typically, a gain of 10,000 was used for the PERG. Amplified signals were acquired with a resolution of 3,096 samples/sec using the Experimenter's Workbench® system (DataWave, Longmont, CO). A 30-sec epoch of PERG responses were recorded and averaged, using 1 second averaging bins. The VisionProbe provided a synchronization signal that ensured the averages were aligned with the counterphase frequency of the gratings. To determine the amplitude of the PERG responses, the averaged data were imported into the PsiPlot V. 7.5 data graphing and analysis software (Poly Software International, Pearl River, NY). The data were subjected to forward Fourier analysis, and the real amplitude component at the counterphase frequency was taken as the response amplitude. For the analysis of PERG recorded after laser exposure, the response phase (in radians) was also obtained.

Results:

a) PERG response as a function of stimulus spatial frequency: Because the PERG is a response due to patterned luminance, and not to a net change of luminance on the retina (Maffei & Fiorentini, 1981), its response amplitude should vary as a function of the spatial frequency of the stimulus. The PERG response consists of an electrical potential generated across the eye by each reversal of the square wave grating. For a counterphased square wave grating, the spatial frequency is expressed as the number of light-dark bars per degree of visual angle, i.e. cycles per degree (cpd). In these experiments, the stimulus spatial frequency was varied from .002 to 14.5 cpd. A composite figure of the PERG responses is shown in Figure 4 for the range of spatial frequencies of 0.01 to 14.5 cpd. Below 0.01 cpd, the stimulus bars were so large that the space-averaged luminance was not zero, and the net luminance change resulted in a luminance ERG response (see below).

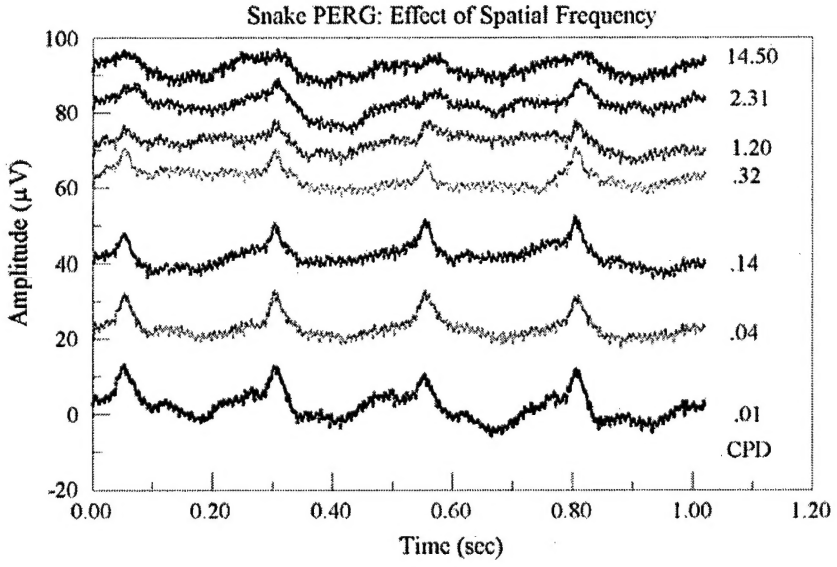

Figure 4. Effect of spatial frequency on the amplitude of the PERG. The PERG waveforms elicited by high (99%) contrast, square wave gratings, presented at the indicated spatial frequencies and at a fixed temporal frequency of 2 Hz, are shown in this composite figure. Each trace was arbitrarily shifted along the amplitude axis for clarity of presentation; the absolute amplitude was not changed.

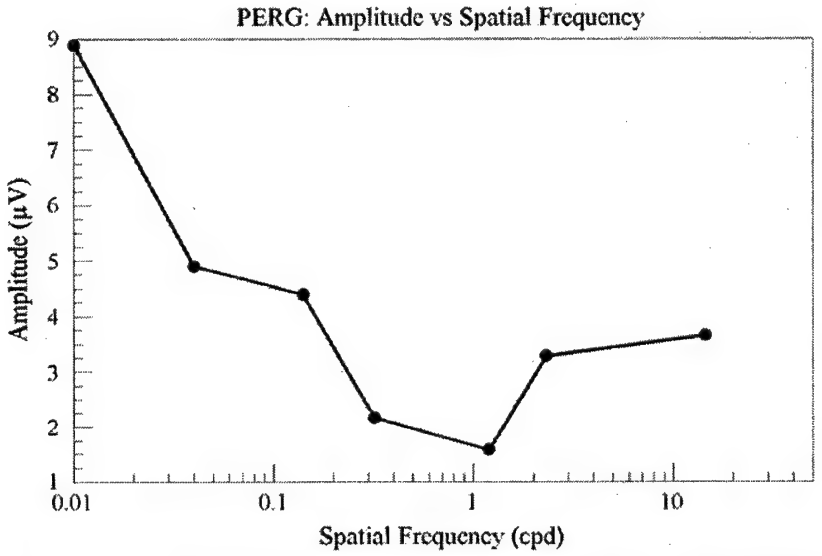

Figure 5: The spatial frequency response function of the PERG in the rat snake. These data were obtained from the waveforms shown in Figure 4. The PERG responses were subjected to Fourier analysis and the amplitude of the frequency component corresponding to the counterphase frequency was determined and plotted in this figure. Although the data are somewhat noisy in the 1-2 cpd region, the function indicates a steadily declining amplitude as the spatial frequency increases, although there is still a recordable response at 14.5 cpd, the highest spatial frequency tested.

The amplitude of the PERG response, elicited by a given spatial frequency, was determined by Fourier analysis. The amplitude of the frequency component corresponding to the counterphase rate was used as the response metric. The spatial frequency response function for a rat snake is shown in Figure 5. The response amplitude falls with increasing spatial frequency, although the small and variable amplitude of the PERG responses obtained with the higher spatial frequencies introduced some noise in the data, i.e. the dip in the function around 1-2 cpd.

b) PERG response as a function of stimulus temporal frequency: As with spatial frequency, the PERG amplitude varies with the temporal frequency of the stimulus. A composite figure, showing the PERG waveforms elicited by stimuli of temporal frequency varied from 1 Hz to 14 Hz, is shown in Figure 6. The snake retina was able to respond to all the stimulus temporal frequencies presented, although the amplitude declined with increasing temporal frequency. This decline may be seen more clearly in Figure 7. The amplitude of each PERG response was determined by Fourier analysis, using the amplitude of the counterphase frequency component as the response metric. Note that the counterphase frequency is distinguished from the temporal frequency. It is the number of pattern "shifts per second", and is nominally twice the temporal frequency of the stimulus, expressed in Hz. As may be appreciated in Figure 7, the PERG amplitude declines as a monotonic function of the temporal frequency.

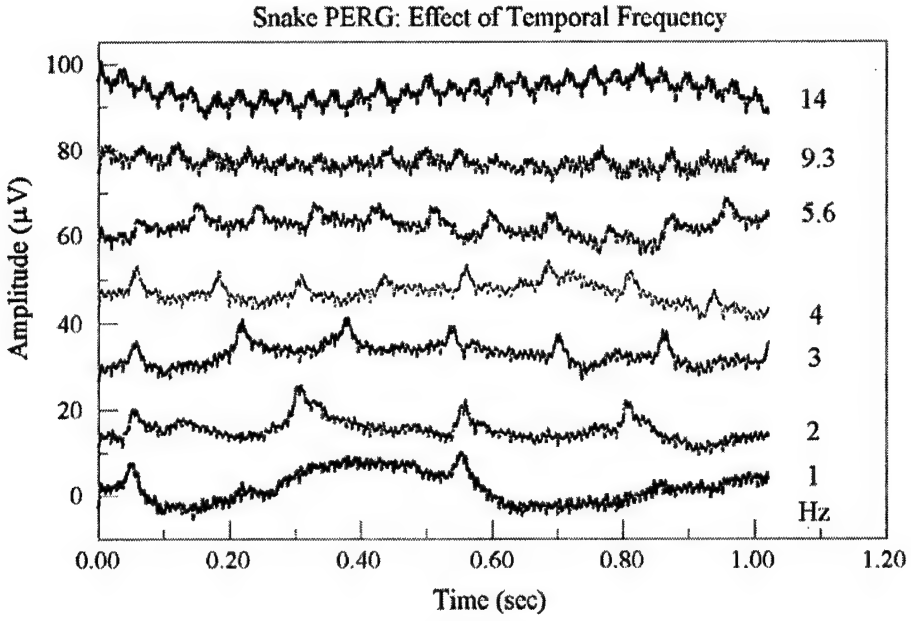

Figure 6: Effect of temporal frequency on the amplitude of the PERG. Each of the waveforms shown in this figure was elicited by a 0.54 cpd square wave grating, presented at the temporal frequencies shown in the figure. The waveforms have been arbitrarily shifted along the Y-axis for clarity.

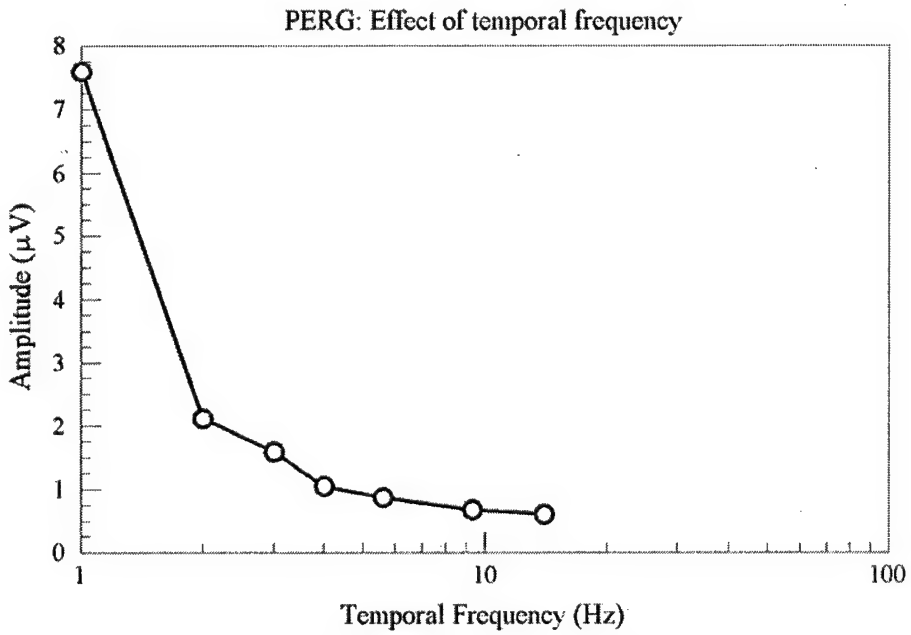

Figure 7: The temporal frequency response function of the PERG in the rat snake. These data were obtained from the waveforms shown in Figure 6, using Fourier analysis to determine the amplitude of the response. The PERG amplitude declines as a monotonic function of the temporal frequency.

c) Focus dependence of the PERG: In order to demonstrate that the PERG was evoked by a change of contrast (i.e., the stimulus pattern) and not by an overall luminance change, an experiment was done in which the stimulus pattern presented on the CRT was defocused by placing a diffuser (a piece of tracing paper) in front of the snake's eye. Two types of stimuli were presented. One was a square wave grating that was of a high enough spatial frequency (0.14 cpd) such that several bars counterphased across the field of view during the test, and the space-averaged luminance of the stimulus did not vary. The diffuser blurred the 0.14 cpd grating nearly completely. If the PERG were solely responding to the pattern, the response should have been abolished by the diffuser. This was indeed the case, as indicated by the upper two traces in Figure 8. In contrast, with a lower spatial frequency stimulus, e.g. the PERG responses to the .002 cpd stimulus shown in the lower two traces in Figure 8, the stimulus bars were so large that there was a net luminance change when they were counterphased. (Each half of the square wave grating nearly filled the entire field of view; when they counterphased, the field alternated between entirely white and entirely black). The diffuser did not abolish this luminance change, and the luminance ERG response was unaffected (lower two traces in Figure 8). This proved that higher spatial frequencies elicit a pattern-specific response, while lower spatial frequencies primarily drive the luminance-sensitive retinal networks.

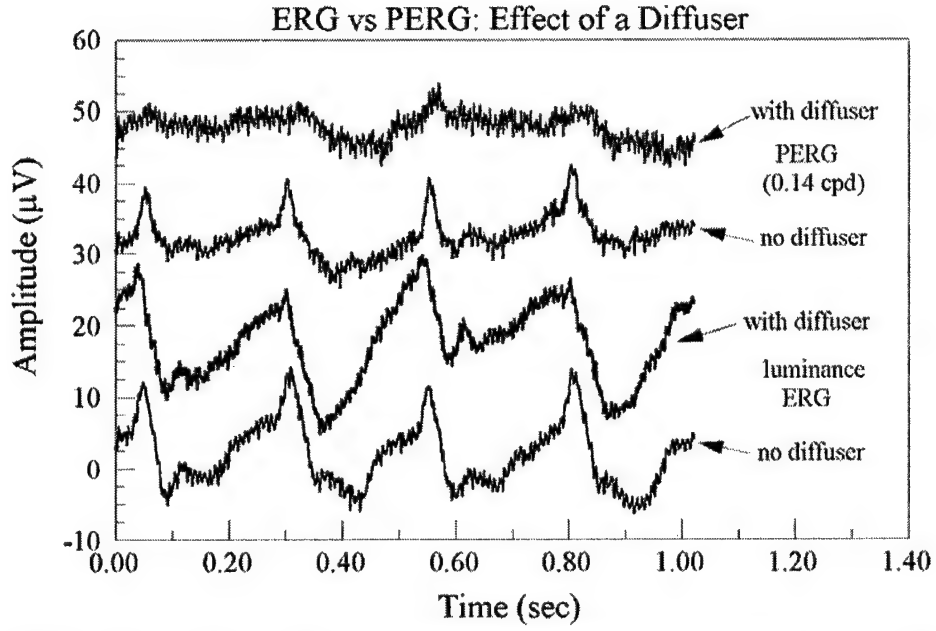

Figure 8: A diffuser placed in front of the snake's eye abolished the PERG response (top two traces), but not the luminance ERG response (bottom two traces). The top two traces were elicited by a 0.14 cpd square wave grating, while the bottom two traces were elicited by a 0.002 cpd grating. See text for additional details.

d) Spectral sensitivity of the snake PERG: Because of conflicting reports of long wavelength sensitivity in related, all-cone snake retinas (Granit, 1943; Jacobs et al., 1992; Sillman et al., 1997), we recorded the PERG response in the rat snake to mid-wavelength visible (green) and long-wavelength visible (red) square wave gratings. Stimuli were presented on the external CRT monitor. The monitor was gamma-corrected prior to recording the stimuli, so that equal luminance stimuli could be presented using the green CRT gun only, followed by the same square wave grating presented with the red CRT gun. In both cases, the stimulus was a 0.54 cpd square wave grating, counterphased at 4 Hz. The response amplitude was determined by Fourier analysis as previously described. In this experiment, the green phosphor elicited a PERG response of 2.10 μV, while the response to the red phosphor stimulus was 1.72 μV (Figure 9). This indicated that the rat snake has considerable sensitivity in the long-wavelength of the visible spectrum, although the greatest sensitivity is probably in the green portion of the visible spectrum.

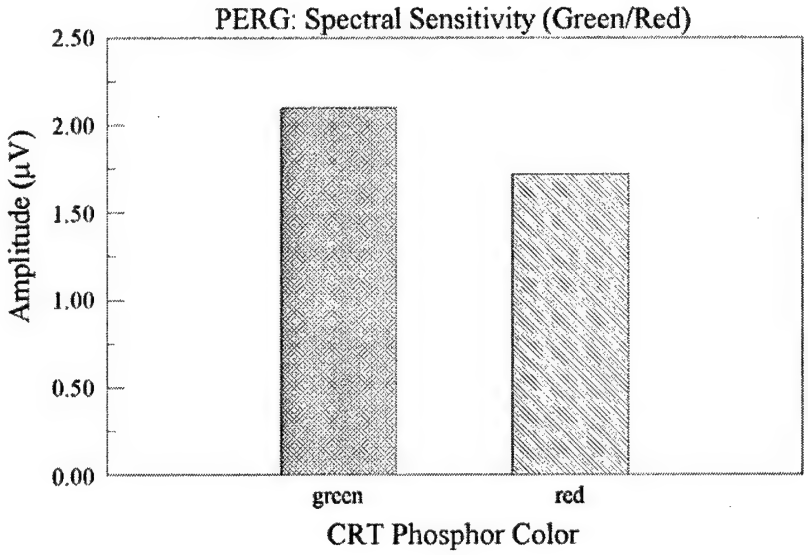

Figure 9: The spectral sensitivity of the PERG in the rat snake. The PERG was elicited by a 0.14 cpd, 4 Hz grating, presented on the CRT. The bar labeled "green" represents the PERG amplitude produced by a green grating, while the other bar shows the PERG amplitude elicited by a red grating.

e) Effect of blue laser on PERG response: The Nd:VO_4 laser initially incorporated into the cSLO imaging system proved to have insufficient output power to produce a permanent lesion in the rat snake. Nevertheless, the laser did have a transient effect on the PERG response, probably due to a flashblinding or, more likely, a local adapting effect on the retina. A typical response to a local laser exposure is shown in Figures 10 and 11. In the experiment illustrated in these Figures, a baseline PERG response was established with a 0.34 cpd, 14 Hz square wave grating (bottom trace in Figure 10). Then, a single, 10-sec exposure was made to the center of the retinal area being stimulated. The laser wavelength was 473 nm, and the total intraocular power was 10 mW. Immediately following the laser exposure, the PERG was recorded for 30 sec (Figure 10, second trace from bottom). Two more PERG records were made over the next two minutes post-laser (Figure 10, upper two traces). Although the response was not abolished by the laser, the stationarity of the response was disturbed. Fourier analysis revealed that the amplitude of the fundamental response was actually increased immediately following the laser, while the response phase was markedly shifted (Figure 11). These changes were consistent with a mildly adapting effect induced by the laser.

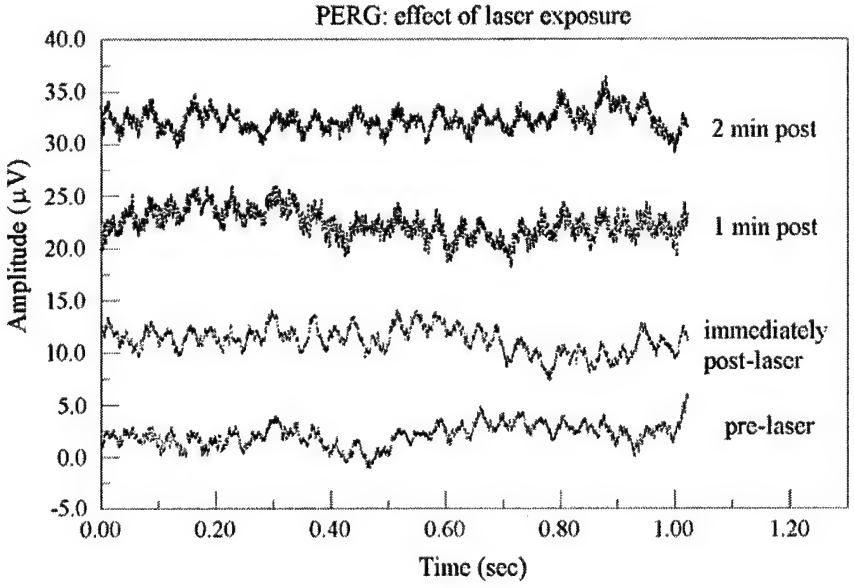

Figure 10: The effect of a laser exposure on the PERG response. A 0.34 cpd, 14 Hz square wave grating was generated with the cSLO. A Nd:VO_4 (473 nm, 10 mW, 10 sec) was aimed at the center of the cSLO field on the retina. The bottom trace in this figure shows the baseline (pre-laser) PERG response in the animal. The second trace from the bottom shows the PERG response obtained immediately after the laser exposure; the third trace from the bottom was obtained 1 min after the laser exposure, and the top trace was obtained 2 min after the laser.

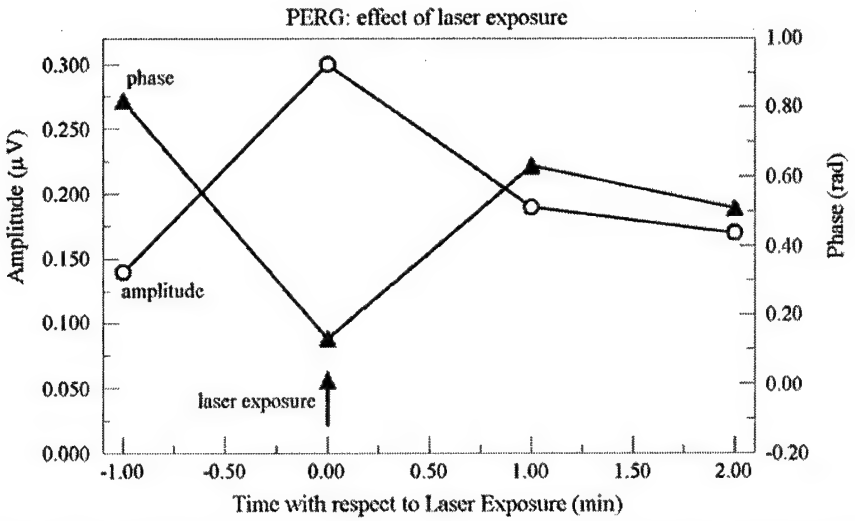

Figure 11: Amplitude and phase of the PERG recorded after a 10-sec laser exposure. Open circles: amplitude data. Filled triangles: phase data. These data were derived from the PERG responses shown in Figure 10. Using Fourier analysis, the amplitude and phase of the responses were determined. The laser exposure caused a transient increase in amplitude, and a 0.6-radian phase lead in the PERG. The responses returned approximately to the baseline by 1 minute post-laser

III. Immunohistochemical analyses of snake retina

The overall focus of our research during this report period was to determine the photoreceptor type of the corn snake (*Elaphe g. guttata*) using immunohistochemical methods. Snakes of the genus *Elaphe* are crepuscular, having scotopic (dim light) vision suggesting rod pigment functions. Based on our research conducted in previous report periods, however, we found (using histological methods) that corn snake retina had cone (photopic) rather than rod (scotopic) cells. In addition, we also studied vitamin A storage in the eye by high performance liquid chromatography (HPLC) and found that most of their retinyl esters are stored in the Retinal Pigment Epithelium (RPE; 0.023-0.500 nmol/eye) rather than in their retina (0.005 – 0.155 nmol/eye). These data suggest that corn snakes have a visual cycle metabolism compatible with a rod-dominated species. To ascertain the issue of cone vs. rod photoreceptor in this species, we have now completed immunohistochemical studies using antibodies specific for cone and rod opsins. Frozen sections of snake eye were incubated with monoclonal antibodies specific for chicken cone opsins (COS-1) and polyclonal antibodies for bovine rod opsin (rhodopsin; B6-30). Control experiments were carried out with chicken (cone-dominated) and bovine (rod-dominated) and these antibodies stained positively with their respective species. Using immunohistochemical methods, corn snake retina reacted positively with antibodies for cone opsins (COS-1) and none with antibodies with rod opsins (B6-30). Therefore, we conclude that corn snakes have cone photoreceptors only. Currently we are using these immunohistochemical methods to study the possible release of TNFα by corn snake retina/RPE upon laser exposure. The positive identification of key proteins in the apoptotic pathway will permit the exploration of new therapeutic agents for laser injury. Frozen sections of

laser induced damaged snake eye were incubated with a monoclonal antibody specific for mouse TNFα. Our preliminary data showed little or no staining suggesting the antigen of interest was either not present or cross reactivity of mouse TNFα did not occur. To ascertain if our above findings are correct, further studies using this antibody of interest on laser induced damaged retina and the development of a positive control are in process.

Methods:

a) Histological examinations: Corn snakes were light adapted and sacrificed with an overdose (300mg/kg) of anesthesia (ketamine / xylazine cocktail, in a ration of 3.5:1 respectively). Eyes were enucleated in light, slit along the anterior chamber and immersed in 2%-2% glutaraldehyde-paraformaldehyde, in 0.087M phosphate buffer (pH 7.2) overnight. Anterior chambers were removed leaving an intact posterior cup for further sectioning. Tissue was washed twice, dehydrated through a series of 50-100% ethanol (ETOH), 1:1 ETOH/ propylene oxide, 100% propylene oxide, 1:1 propylene oxide/epon and 100% epon. Tissue was then oriented in capsules and allowed to polymerize in an oven at 63^0 C for 15-30 hours. An ultra-microtome was used to obtain 1-2 μm sections which were then applied to microscopic slides, heat dried and stained with 0.5% Toluidine-Blue before viewing under a light microscope.

b) Antibodies: Cone-specific monoclonal antibody COS-1 produced against photoreceptor membranes of the chicken is specific for long and middle wavelength pigments of cone outer segments and recognizes the C-terminal portion of the last six amino acids (Szel & Rohlich, 1985; Rohlich & Szel, 1993). COS-1 has also been shown to label middle and long-wavelength-sensitive cones in tetra pods (Szel et al., 1986; Rohlich & Szel, 1993) as well as Large Single and Double cones of the garter snake (*Thamnophis sirtalis*; Sillman et al., 1997). We have obtained this antibody from Dr. Rohlich (in Budapest). In addition, we were able to obtain a rod specific antibody against bovine rhodopsin (B6-30) from Dr. Hargrave (in Florida). Prior to applying these antibodies to corn snake retina, we applied each antibody to a cone-dominated (chicken) versus a rod-dominated species (bovine) to test the specificity of each antibody. These results serve as positive controls and verification of the efficacy of our immunohistochemical methods.

c) Immunohistochemistry in chicken and bovine eyes: Several eyes were enucleated of each species and the anterior chambers removed, leaving the RPE and retina intact. Tissue was immediately immersed in liquid nitrogen, embedded in OCT compound medium (-23°C), cryo-sectioned (10μm) and applied on to microscopic slides (Poly-L-Lysine coated) for storage at –85° C. Upon removal, sections were air dried, immersed in 4% paraformaldehyde with 3% sucrose in 0.087M phosphate buffer (pH 7.5) for 30min, washed, incubated in .3% hydrogen peroxide (10min), washed, immersed in blocking serum (30min), and then exposed overnight to the cone specific monoclonal antibody COS-1 using a dilution of 1:40. Labeling of the primary COS-1 was achieved using Vector Laboratories' *Vectastain elite ABC-Peroxidase* kit along with 3,3'-diaminobenzidine (DAB) as a substrate. Tissue structure and DNA were counter-stained using Sigma's *Harris hematoxylin and eosin.* Visualization of antibody and morphology were obtained under a light microscope.

When using an elite ABC-Peroxidase kit, the primary antibody is attached to a biotinylated secondary antibody then to an Avidin, Biotin enzyme complex. When incubated with a substrate such as DAB in this study, it precipitates a brownish color reaction showing positive labeling of the primary antibody (Figure 12).

d) Immunohistochemistry in corn snake eyes: Several animals were sacrificed with an

overdose (300mg/kg) of anesthesia (ketamine / xylazine cocktail, in a ration of 3.5:1 respectively). The eyes were enucleated and the anterior chambers removed, leaving the RPE and retina intact. Tissue was immediately immersed in liquid nitrogen, embedded in OCT compound medium (-23°C), cryo-sectioned (10μm) and applied on to microscopic slides (Poly-L-Lysine coated) for storage at –85° C. Upon removal, sections were air dried, immersed in 4% paraformaldehyde with 3% sucrose in 0.087M phosphate buffer (pH 7.5) for 30min, washed, immersed in blocking serum (30min), and then exposed overnight to the cone specific monoclonal antibody COS-1 using a

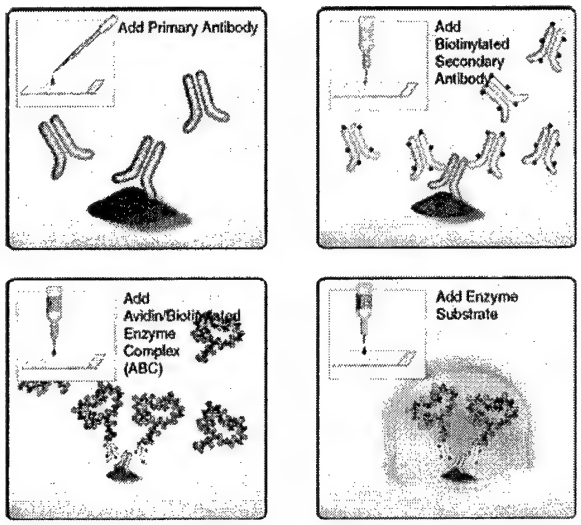

Figure 12: Vectastains elite ABC-Peroxidase reaction

dilution of 1:40. Parallel sections were also exposed to B6-30 antibody using a dilution of 1:50. Visualization of tissue labeling was achieved using secondary antibodies conjugated to the fluorescent Texas Red (excitation 596nm, emission 620nm) before viewing under a fluorescent microscope. ABC Peroxidase kits were not used in snake retina due to difficulty of visualization of its brown color from the dark RPE background (see additional explanations in results).

Results:

a) Histological data on the corn snake retina (Figures 13 A&B): As we have previously reported, the corn snake's retina contains photoreceptor cells, which exhibit cone-type morphology with short round outer segments. Based on these photomicrographs, no rod photoreceptors were identified. These photos are presented as a reference to the photomicrographs from immuno-histochemical studies with less morphological details (Figures 14 and 15).

b) Immunohistochemistry in chicken and bovine controls: Figures 14 A and B show photomicrographs depicting the labeling of COS-1 (cone opsin-specific) antibody for chicken eye (cone-dominated). Figure 14A shows that COS-1 antibody positively stained the outer segment layer (see brown color layer adjacent to the black color RPE layer) where cone opsin resides. In

comparison, Figure 14B shows that the control (thin section incubated with buffer in place of COS-1 antibody) did not exhibit any (brown color) immunostaining. These results confirmed that the COS-1 antibodies recognized the chicken cone opsin and that our immunohistochemical method, using this COS-1 antibody, is appropriate to demonstrate the presence of chicken cone opsin.

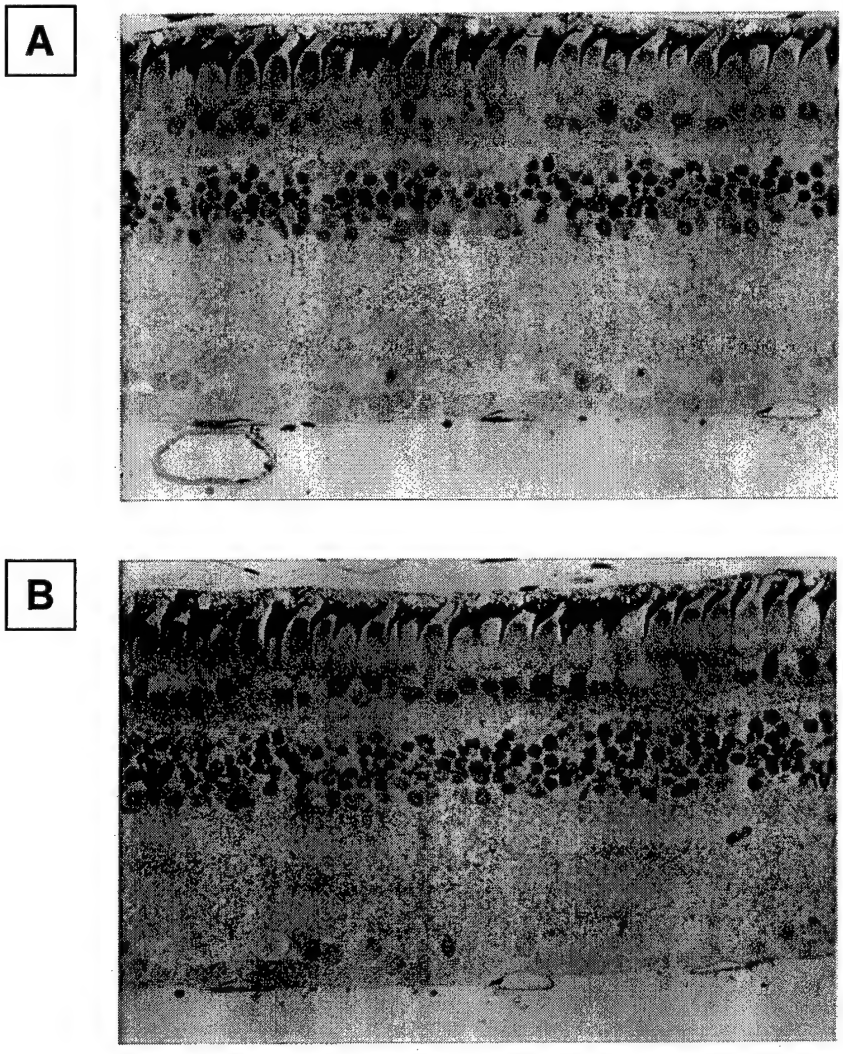

Figure 13 A&B: Cross section of the retina from the rat snake (*Elaphe g. guttata)* inner retina at the bottom, outer retina toward the top w/photoreceptors (w/ adherent REP pigment) in the uppermost strata.

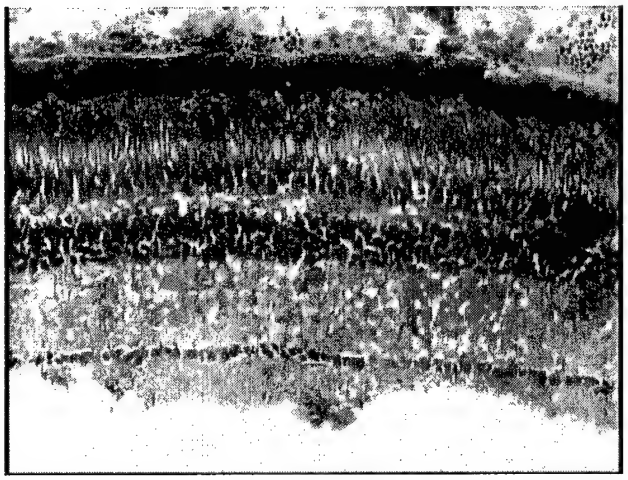

Figure 14A: Chicken retina labeled with COS-1 antibody

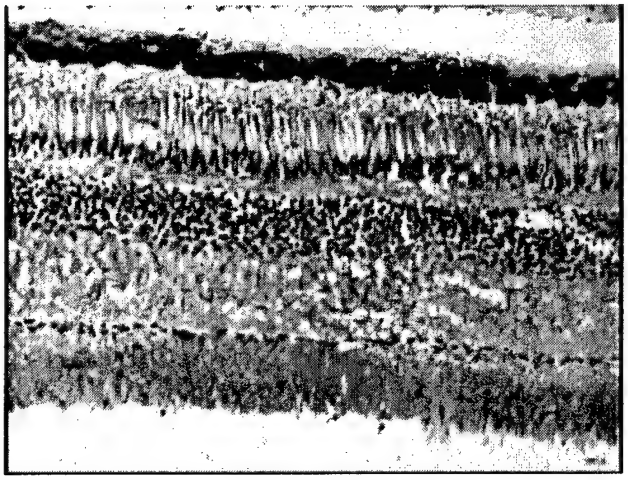

Figure 14B: Negative control, chicken retina without COS-1

Figures 15 A and B show photomicrographs indicating the labeling of B6-30 (rod opsin-specific) antibody for the bovine eye (rod-dominated). Figure 15A shows that B6-30 antibody positively stained the outer segment layer (see brown color layer) where rod opsin resides. In comparison, Figure 15B shows that the control (thin section incubated with mouse non-immune serum in place of immune serum containing B6-30 antibodies) did not exhibit any (brown color) immunostaining. These results confirmed that B6-30 antibodies recognized the bovine rod opsin and that our immunohistochemical method, using this B6-30 antibody, is appropriate to demonstrate the presence of bovine rod opsin.

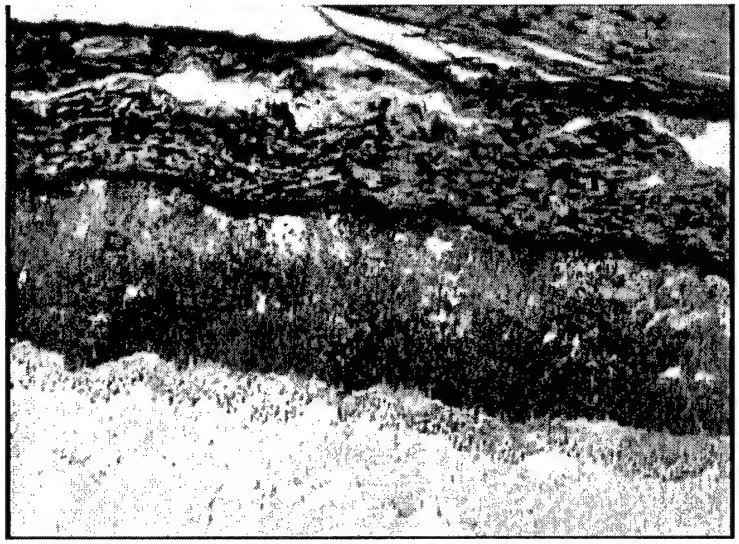

Figure 15A: Bovine retina labeled with B6-30 antibody

c) Immunohistochemistry in corn snake eyes: We first attempted to apply COS-1 and B6-30 to immunostain the cryo-sections prepared from corn snake eyes, using the ABC peroxidase substrate reaction as indicated above. However, the photomicrographs were difficult to interpret, as the corn snake's photoreceptors were deeply embedded in its RPE, so that the positive stain (brown), if any, was masked by the dark (black) melanin of the RPE (see Figure 16 below).

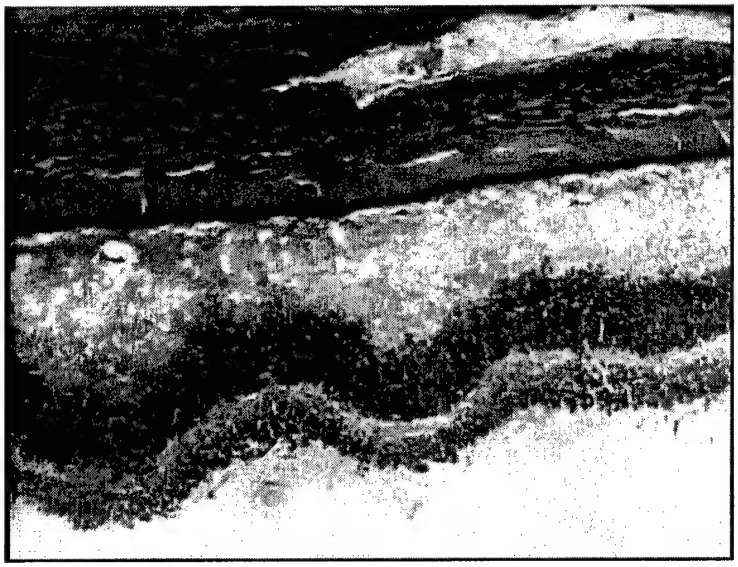

Figure 15B: Negative control Bovine retina without B6-30 antibody

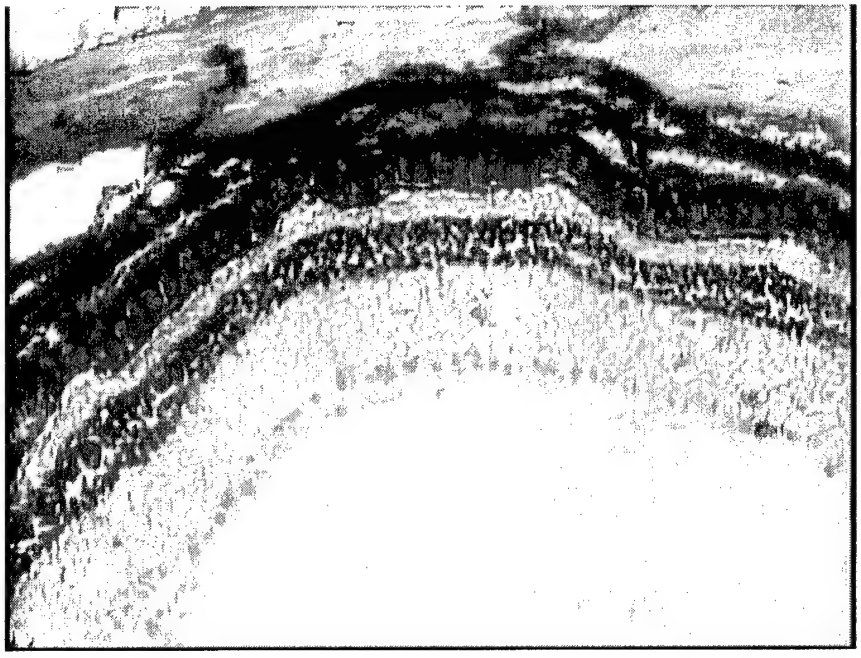

Figure 16: Snake retina labeled with COS-1 antibody and visualized using an ABC peroxidase reaction.

Based on this observation, we changed the method of visualization of the primary antibody. Instead of using a secondary antibody conjugated to peroxidase (developing a brown color), we used a secondary antibody conjugated to a fluorescence dye (Texas Red; excitation 596nm, emission 620nm) to visualize fluorescence instead of color staining. Figure 17A shows a photomicrograph of red fluorescence in corn snake eye cryo-section incubated with COS-1 antibody. The red band indicates that this cone-specific antibody has bound to the snake photoreceptors indicating that these cells contain cone pigments with epitopes similar to those of the chicken cone opsins. Our observation is consistent with published data that COS-1 developed from chicken cone membrane, cross reacts with other snake cone photoreceptors (Rohlich & Szel, 1993). Our control section, incubated with buffer in place of primary antibody, did not reveal any red fluorescence (Figure 17B). Based on these observations, we conclude that corn snakes possess cone pigments in their photoreceptors.

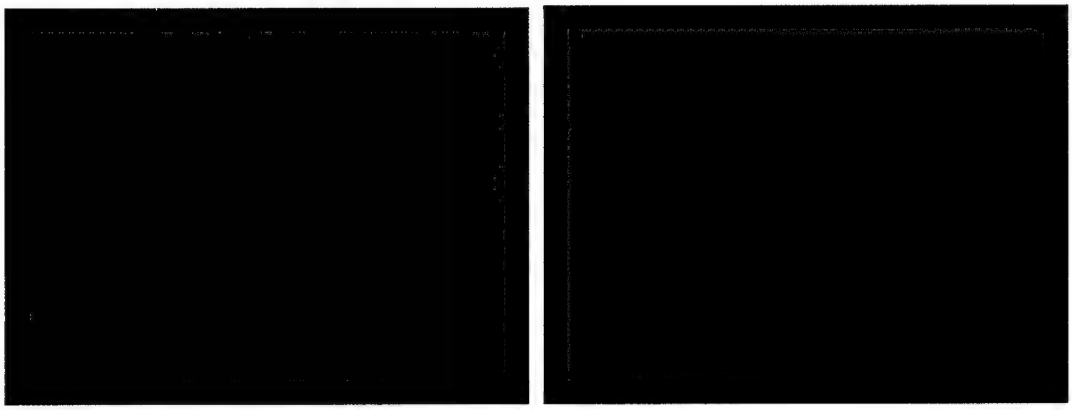

Fig.17A: Snake retina labeled with COS-1 antibody visualized using Texas Red fluorescent.

Fig.17B: Negative control, snake retina without COS-1 antibody

Figures 18 A and B show fluorescence photomicrographs of corn snake eye cryo-sections incubated with B6-30 antibodies. The lack of red fluorescence band in both the experimental (Figure 18A: incubated with B6-30) and the control (Figure 18B: incubated with mouse non-immune serum in place of serum containing B6-30 antibody) strongly suggests that the rod pigment rhodopsin is not found in the corn snake photoreceptors. This suggests that corn snakes do not possess any rod cells with rhodopsins. However, this is based on the assumption of cross reactivity of B6-30 antibody between bovine and snake rhodopsin.

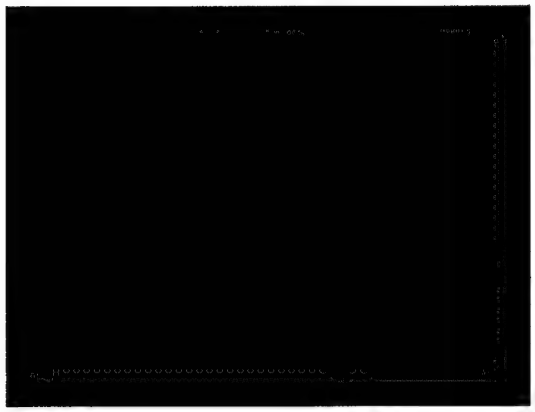

Fig. 18A: Snake retina labeled with B6-30 antibody and Texas Red fluorescent.

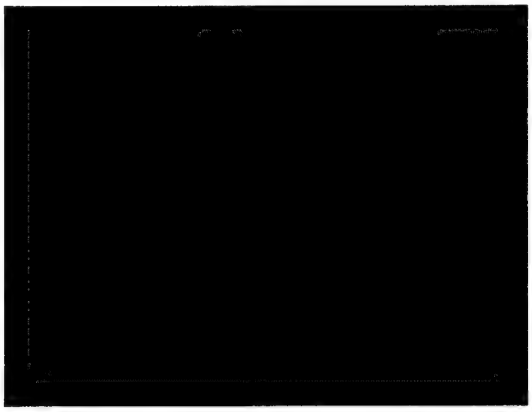

Fig. 18B: Negative control, snake retina without B6-30 antibody

KEY RESEARCH ACCOMPLISHMENTS

- Experiments were conducted to determine exposure parameters for producing photochemical lesions in the rat snake. Even with the best-determined parameters, photochemical lesions do not appear observable beyond much more than one day post-exposure, and therefore are not well suited for longitudinal studies of treatment effects.
- Experiments with histochemical marker dyes and N-Acetylcysteine (as treatment) were done in subjects, which received photochemical lesions, to compare the resultant effects to animals in a previous study, which had received thermal retinal lesions. However, the lack of observable permanent cellular deficits in subjects of the present study did not leave experimental end points to be improved by treatment, or for comparison of photochemical with thermal retinal lesions in the rat snake.
- Several experiments were done to characterize the basic physiology of the pattern-evoked electroretinogram (PERG) response in the rat snake retina, and the functional characteristics of PERG recorded from the normal snake eye have been documented.
- Results of eliciting the PERG by spatial or temporal frequencies further support the idea that the rat snake has cone photoreceptors, even though it is a crepuscular species.
- Using the PERG to test the spectral sensitivity of the rat snake retina resulted in good photopic sensitivity across most of the visible spectrum, if not the ability to distinguish red/green color contrast.
- The PERG was successfully recorded to demonstrate an overall retinal function change subsequent to a subthreshold retinal lesion.
- Immunohistochemical examinations have successfully demonstrated that the photoreceptors of rat snakes label with cone specific antibody. This is further evidence that rat snake's retina is exclusively cone and not rod.

REPORTABLE OUTCOMES

Presentations:

- Elliott, W.R., Glickman, R.D., Rentmeister-Bryant, H., & Zwick, H. (2004). Functional assessment of snake retina using pattern ERG. Presented at the 1st annual CBST Biophotonics Symposium, University of Texas Health Science Center, San Antonio, TX

- Leal, R., Tsin, A., Glickman, R., Elliott, R., & Rentmeister-Bryant, H. (2004). Ocular retinoids and photoreceptors in Corn snake (*Elaphe g. guttata*). Presented at the 1st annual CBST Biophotonics Symposium, University of Texas Health Science Center, San Antonio, TX

- Elliott, W.R., Rentmeister-Bryant, H, Barsalou, N., Beer, J., & Zwick, H. (2004). N-Acetylcysteine and acute retinal laser lesions in the colubrid snake eye. In: Laser Interaction with tissue and cells XV, Jacques, S.L., & Roach, W.P. (eds.), Proceedings of SPIE 5319-45, 267-273.

Training supported by this award:

Robert Leal is a graduate student in the Biology MS (with thesis option) program at UTSA. He is currently performing the immunohistochemical analyses of TNFα released in corn snake retina post laser insult, and performed the immunohistochemical work for this reporting period. He is supported by the NETP since spring 2002.

Funding applied for based on work supported by this award:

Project Title: "Do therapeutic applications of antioxidants in laser eye injuries work? A test of effectiveness using the transcription factor NF-kB in the snake model."

Funding Category applied for: NHRC In-House Laboratory Independent Research

Funding result for FY04: The proposal was funded ($140K).

CONCLUSIONS

This project's main objective is to develop an *in vivo* damage model for the study of the mechanisms underlying retinal injuries (e.g., due to laser exposure) and other neurodegenerative disorders. For this purpose we have selected the snake eye with its unique suite of ocular properties, combined with the imaging capabilities of the confocal Scanning Laser Ophthalmoscope. This model needs fewer animals, requires less euthanasia, and uses a lower order animal than similar experiments with rodents. The snake eye is also one of the few small animal ocular models with an all cone photoreceptor retina, and may be so more applicable to human macular disease/injury than rodent or rabbit models that have rod-dominated eyes.

In order to establish this model for the study of neurodegeneration and human disease, we must continue to study the properties of the snake eye as well, and find the similarities and differences between snake and human vision.

Except for the morphological studies on photochemical retinal lesions, the work performed in the present work period has confirmed and extended our previous findings. The all-cone photoreceptor complement of the retina has been confirmed by immunohistology, and the functional characteristics of PERG recorded from the normal snake eye have been documented. Initial experiments with laser exposures were done, which indicate that the PERG is capable of tracking laser-induced changes in function.

In the primate retina, the PERG is primarily photopic in origin (Maffei & Fiorentini, 1990), implying it is generated from cone photoreceptor pathways. In the cat retina, however, the PERG appears to be generated by cone and rod photoreceptors (Maffei & Fiorentini, 1982; Shuurmans & Berninger, 1984), a result, perhaps, of the large rod contribution to retinal function in the cat. Similar to findings in primates (Maffei et al., 1985), optic nerve section in the cat causes decrement of the PERG (Maffei & Fiorentini, 1981; Hollander et al., 1984), consistent with the contribution of ganglion cell responses to the PERG. Snakes may present examples of exclusively photopic PERG responses, as well as those with both photopic and scotopic components, because some species have exclusively cone retinas, e.g. the colubrids, while other species have mixed rod/cone retinas, e.g. the crotalids (Underwood, 1970). Therefore, it was of interest to characterize the basic physiology of the PERG response in the rat snake (a colubrid).

According to anatomical studies on the closely related garter snake, *Thamnophis sirtalis*, (Sillman et al., 1997), the retina is composed of all-cone photoreceptors. While the density of photoreceptors in the snake retina does not approach that of primates and other truly foveated retinas, the snake retinal matrix is dense enough to subserve better visual acuity than many mammals. For example, in the dog, the PERG can be elicited by spatial frequencies from 0.015 to 1.92 cpd (Sims & Ward, 1993). In the present work, a 14.5 cpd stimulus pattern was found to produce a still-recordable PERG response. Thus, in the dog, the maximum acuity is about 15 minutes of arc, while the rat snake may be able to resolve 2-3 minutes of arc visual angle.
The all-cone retina of the snake should also be able to follow high stimulus rates, due to the fast temporal response of cone photoreceptors. The rat snake PERG easily responded to a 14 Hz stimulus, the fastest frequency tested. This frequency is at or above the typical cutoff flicker frequency of human rods (Birch, 1991). It should be noted that the PERG is actually responding at the counterphase rate, which for the 14 Hz (temporal frequency) grating, corresponds to 28 pattern shifts per second. In the garter snake, flicker ERG responses were recorded in excess of 62 Hz (Jacobs et al., 1992). Although such a high stimulus temporal frequency was not tested in the rat

snake, it appeared from the temporal frequency response function (Figure 7), that the PERG would likely be extinguished before reaching such a high temporal frequency. This "intermediate" performance of the rat snake cone photoreceptor may be consistent with the adaptation of this animal's visual system to its crepuscular lifestyle (active at dawn and dusk); an hypothesis that was advanced earlier, based on the biochemical profile of the cone visual pigments in the closely related corn snake (Leal et al., 2002), as well as the temporal response characteristics of the PERG (Elliott et al., 2003).

Early single unit recordings from the retina of the snake, *Tropidonotus natrix*, a somewhat related species, found evidence for mid-wavelength ("green") and long-wavelength ("red") receptors, with wavelength maxima at 560 nm and 600 nm, respectively (Granit, 1943). No blue receptors were found. In *Thamnophis*, only a single, broadly peaked spectral mechanism was found, using the flicker ERG as the measure (Jacobs et al., 1992). This spectral sensitivity declined sharply below 450 nm and above 650 nm. By microspectrophotometry, *Thamnophis* was found to have a mid-wavelength receptor at 554 nm, and two short-wavelength receptors, one at 482 nm, and the other in the UV band at 360 nm (Sillman et al., 1997). It is curious that no long-wavelength receptor was found. Despite the lack of anatomical evidence for long-wavelength receptors, in the present study the amplitude of the PERG response to a long wavelength stimulus was 80% of that elicited by a mid-wavelength stimulus. This is consistent with the findings of Jacobs et al. (1992), and suggests that the spectral sensitivity of the "green" receptor in these snakes is very broad, giving the animal good photopic sensitivity across most of the visible spectrum, if not the ability to distinguish red/green color contrast.

Although the laser employed in the present study was not powerful enough to produce a lesion (which is still a central goal of these investigations), it evidently was intense enough to induce a change in overall retinal function. These changes were manifested by shifts in the amplitude and phase of the PERG. The increase in amplitude of the PERG immediately after the laser exposure was counter to expectation; if "flashblindness" was induced by the laser, the response of the retina should have been reduced (Glickman, 1987; 1989). The result may instead be due to disinhibition of the PERG response. The site of laser impact was much smaller than the retinal area stimulated by the counterphasing gratings. The adapting effect of the laser at one site could have caused release from lateral inhibition at distant sites, resulting in a transient increase in PERG amplitude. The unlocking of the phase of the main response component is also consistent with this hypothesis.

Future work will explore the effect of suprathreshold laser exposures. With the installation of a Nd:YAG laser capable of delivering much higher retinal irradiance, the effect of retinal lesions on the PERG response may proceed.

Based on our immunohistochemistry data with COS-1 antibody, corn snake retinas contain cone opsin therefore, cone photoreceptors. Using B6-30 antibodies for bovine rhodopsin, we were unable to confirm the existence of rod pigment (rhodopsin) in the corn snake retina. This suggests that corn snakes may contain cone-only retinas. This conclusion is consistent with our early histochemical analyses that corn snake retina contain photoreceptor cells exhibiting only cone morphology. However, our biochemical analyses on vitamin A shows a higher presence of esters within the corn snakes' RPE versus its retina, which is atypical of a cone-dominated species (Nathan et al., 2002) and is found mostly in rod-dominated species. Overall, it is possible that this species has evolved over time and adapted to its environment producing a type of photoreceptor that functions bi-modally as a rod and a cone.

Based on these results, the immunohistochemical methods offer a new approach to study the mechanism and the prevention of laser-induced eye injury. This is because antibodies for key proteins in laser-induced apoptosis (programmed cell death) in the eye are commercially available and our immunohistochemical method can detect minute quantities (in comparison to extraction and then determination by ELISA). Such proteins can be tested on cryo-sections of the snake eye to reveal if they are secreted in response to laser exposure. We are now testing if TNFα (a protein in the apoptotic pathway) is released by corn snake retina/RPE upon laser exposure. Animals tested were sacrificed five hours and twenty- four after being exposed to laser injury and processed using the immunohistochemistry methods listed above. Frozen sections were then incubated with a monoclonal antibody specific for mouse TNFα and visualized for fluorescence to indicate positive staining. Upon visualization sections showed little or no staining indicating the antigen of interest (TNFα was not present or the antibody we used has no cross reactivity within snake tissue). We plan to conduct further tests on these sections and develop a positive control to un-equivocally identify proteins expressed in the apoptotic pathway and then explore new therapeutic methods for the effective prevention and/or treatment of laser-induced eye injury

REFERENCES

Birch, D.G. (1991). Flicker electroretinography. In: Principles and practice of clinical electrophysiology of vision, Heckenlively J.R., & Arden G.B. (eds.), St. Louis: Mosby Year Book, chap 45, pp 348-351.

Elliott,W.R., Glickman, R.D., Rentmeister-Bryant, H., & Zwick, H. (2003). Functional assessment of snake retina using pattern ERG. Invest. Ophthalmol. Vis. Sci., 44 E-abstract 2706.

Glickman, R.D. (1987). Differential effects of short- and long-pulsewidth laser exposures on retinal ganglion cell response. Lasers in Surgery and Medicine, 7, 434-440.

Glickman, R.D. (1989). Prolonged activity of retinal ganglion cells following intense, nanosecond laser flashes. Clin. Vision Sci., 4,1-18.

Granit, R. (1943). "Red" and "green" receptors in the retina of *Tropiodonotus*. Acta phys. Scandinav. , 5,108-113.

Hollander, H., Bisti, S., Maffei, L., & Hebel, R. (1984) Electroretinographic responses and retrograde changes of retinal morphology after intracranial optic nerve section. A quantitative analysis in the cat. Exp. Brain Res., 55, 483-493.

Jacobs, G.H., Fenwick, J.A., Crognale, M.A., & Deegan, J.F II. (1992). The all-cone retina in the garter snake: spectral mechanisms and photopigment. J. Comp. Physiol. A ,170, 701-707.

Leal, R., Tsin, A., Glickman, R., Elliott, R., & Rentmeister-Bryant, H. (2002). Ocular retinoids in Cornsnake (*Elaphe g. guttata*). Invest.Ophthalmol. Vis.Sci., 43, E-abstract 3602.

Maffei, L., & Fiorentini, A. (1981). Electroretinographic responses to alternating gratings before and after section of the optic nerve. Science, 211, 953-955.

Maffei, L., & Fiorentini, A. (1982). Electroretinographic responses to alternating gratings in the cat. Exp. Brain Res., 48, 4327-4334.

Maffei, L., & Fiorentini, A. (1990). Pattern visual evoked potentials and electroretinograms in man and animals. In: Visual Evoked Potentials, Desmedt, J.E. (ed.), New York: Elsevier Science, pp 25-33.

Maffei, L., Fiorentini, A., Bisti, S., & Hollander, H. (1985) Pattern ERG in the monkey after section of the optic nerve. Exp. Brain Res., 59, 423-425.

Nathan, L., Mata, R., Radu, A., Clemmons, R., & Travis, G.H. (2002). Isomerization and Oxidation of Vitamin A in Cone-Dominant Retinas: A Novel Pathway for Visual pigment Regeneration in Daylight. Neuron, 36, 1-20.

Rentmeister-Bryant, H., Glickman, R., Tsin, A., & Elliott, R. (2002) Evaluation of chronic stress induced neurodegeneration and treatment using an *in vivo* retinal model. DAMD-TR-2002-1443.

Rentmeister-Bryant, H., Glickman, R., Tsin, A., & Elliott, R. (2003) Evaluation of chronic stress induced neurodegeneration and treatment using an *in vivo* retinal model. DAMD-TR-2003-in press.

Rohlich, P., & Szel, A. (1993). Binding sites of photoreceptor-specific antibodies COS-1, OS-2 and Ao. Current Eye Research, 12, 935-944.

Schuurmans, R.P., & Berninger, T. (1984). Pattern reversal responses in man and cat: A comparison. Ophthalmic Res., 16, 67-72.

Sillman, A.J., Govardovskii, V.I., Röhlich, P., Southard, J.A., & Loew, E.R. (1997). The photoreceptors and visual pigments of the garter snake (*Thamnophis sirtalis*): a microspectrophotometric, scanning electron microscopic and immunocytochemical study. J. Comp. Physiol. A, 181, 89-101.

Sims, M.H., & Ward, D.A. (1993). Response of pattern-electroretinograms (PERG) in dogs to alterations in the spatial frequency of the stimulus. Prog. Vet. Comp. Ophthalmol., 3, 106-112.

Szel, A., & Rohlich, P., (1985). Localization of visual pigment antigens to photoreceptor cells with different oil droplets in the Chicken retina. Acta Biol Hung, 36(3-4), 319-24.

Szel, A., Takacs L., Monostori, E., Diamantstein, T., Vigh-Teichmann, I., & Rohlich, P. (1986). Monoclonal antibody-recognizing cone visual pigment. Exp Eye Res, 43, 871-883.

Underwood, G.. (1970). The eye. In: Gann, P., & Parsons, T.S. (eds.), Biology of the Reptilia, vol. 2. New York: Academic Press, pp 76-97.